Springer

Journal of Mechanical Science and Technology 23 (2009) 1680~1692

Journal of
Mechanical
Science and
Technology

www.springerlink.com/content/1738-494x
DOI 10.1007/s12206-009-0419-z

Spray formation by like-doublet impinging jets in low speed cross-flows †

S. S. Lee[1], W. H. Kim[2] and W. S. Yoon[2,*]

[1]*Korea Military Academy, Seoul, Korea 139-799*

[2]*Department of Mechanical Engineering, Yonsei University, Seoul, Korea 120-749*

(Manuscript Received August 1, 2008; Revised March 30, 2009; Accepted April 1, 2009)

Abstract

Breakup and spray formation by impinging liquid jets introduced into a low-speed cross-flow are experimentally investigated. Effects of the cross-flows on the macroscopic and microscopic spray parameters are optically measured in terms of jet Weber number and liquid-to-gas momentum ratio. The liquid stream undergoes Rayleigh jet breakup at lower jet Weber numbers and bag/plume breakup at higher momentum ratio through Kelvin-Helmholtz instability. In particular, the first and the second wind breakup occur at an intermediate jet Weber number. At higher jet Weber numbers, the hydrodynamic impact waves commands and the effect of the convective gas flows is insignificant. The breakup length rises in proportion to the jet Weber number, but starts to decrease when the jet Weber number further rises over 1000. The cross-flow promotes the jet breakup and renders a finer spray in an entire range of injection velocities.

Keywords: Spray; Jet Impingement; Like-doublet; Cross-flow

1. Introduction

An atomization is considered as a disruption of the consolidating influence of surface tension by the action of internal and external forces. In the event of an injection into a stagnant atmosphere, the liquid stream commands the disintegration and the transport of the mass, momentum, and energy between the gas and liquid depends solely on the dynamic characteristics of the liquid stream. The injection into a convective gas flow, however, yields vastly different spray formation. When the gas flow is hindered by the traversing liquid jet, the aerodynamic force acting on the liquid surface promotes the disruption by adding an external distorting force. Activation of the atomization is concomitant with augmentation of the momentum exchange and the wave energy. Application of this convection-assisted atomization is diverse in the industry. Fuel sprays in turbojet, ramjet, scramjet combustors [1-7] and urea injection into automobile exhaust for a diesel NO_x after-treatment [8] are representative. In these applications, the cross-flow naturally occurs in the course of breathing or exhausting the gas, hence the atomization quality can be improved with no additional expense.

In-depth macroscopic studies on the spray formation in a cross flow have been made and generally focused on elucidating the spray appearance, penetration heights, velocity fields, and effects of liquid property [1-5]. Both sub- and supersonic cross-flows were examined, and the breakup mechanism of the single liquid jet was experimentally investigated. Instant shadowgraph pictures showed that the liquid column breakup resembles the secondary breakup of a spherical droplet flying in a stagnant gas [3]. The somewhat quantitative nature of the jet column fracture was also addressed in view of the wave parameters. The images showed that the surface waves of large amplitude propagating on the liquid jet at a sizable velocity of an order of the injection velocity rule

† This paper was recommended for publication in revised form by Associate Editor Gihun Son

*Corresponding author. Tel.: +82 2 2123 4812, Fax.: +82 2 312 2159
E-mail address: wsyoon@yonsei.ac.kr

the jet integration [2]. Experiments on the microscopic spray structure were also conducted for the cross–sectional spray distributions, centerline properties, flux-averaged properties, and spray correlations were proposed [2]. Dai et al. [9] studied the secondary breakup of a droplet by shock wave disturbances concurrent with supersonic flow interruption. Primary breakup of a round non-turbulent liquid jet in the gaseous cross-flows was visually shown by using pulsed shadowgraph and holograph technique. Qualitative similarities between the primary breakup of non-turbulent round liquid jets in gaseous cross-flows and the secondary breakup of drops subjected to shock wave disturbances were demonstrated.

Parametric studies on the spray characteristics provide better understanding of the spray dynamics as well as a database for the development of spray control technology. Jet breakup, liquid column trajectories and distances to column fracture points were measured in terms of injection liquids, injector diameters, and air Mach numbers [3]. Effects of injection parameters on the breakup of turbulent liquid jets in subsonic cross-flows were optically measured [4-5]. Comprehensive experimental studies on the penetration and the breakup of the liquid jets injected normal to high-Mach subsonic airstreams through injection ports of various geometries and sizes provided the correlations of the jet penetration to essential injection parameters [1]. Recently, a computational study on the surface wave and the deformation of non-turbulent round liquid jet situated in uniform gaseous cross-flows was attempted [7].

These early studies focused on the spray formation of a plain liquid jet injected from a single circular or non-circular orifice. The plain injector incorporated with a single orifice element highly fulfills essential injector requirements such as manufacturability and controllability. But the single-orifice injection method is not well fit for generating a fine spray because of high injection pressure, which is frequently inadequate for the system or costly.

An impinging element produces two liquid streams that impinge at a given angle at a prescribed distance from the injector face. Impact waves caused by the jet impingement act to break up the liquids. The liquid sheet is disintegrated intermittently while it generates groups of drops and propagates showing wavelike expansion from the point of impingement. Formation of a fanlike elliptical liquid sheet in the perpendicular direction to the plane of the impinging jets results (Fig. 1). Over decades, usefulness of the impinging jets has been demonstrated in diverse applications such as numerous storable-propellant engines, small reaction control thrusters, and even a car-washing sprayer. Its geometric simplicity and relative ease of fabrication present the impinging injector as a system- and cost-effective alternative to two-fluid atomizers. In particular, two of the aforementioned industrial applications, the ramjet and scramjet combustor, employ the impinging jets situated in crossing gas flows. Typically, the heavy-thrust requirement in these super- and hypersonic air-breathing engines is fulfilled by the impinging injection method for a massive supply of the liquid fuel but with minimum pressure loss.

Numerous reports regarding the macroscopic spray characteristics of the impinging jets have been issued, but the studies on the microscopic characteristics are few since high-resolution measurement became available lately. Characteristic frequencies and droplet size caused by like-doublet jet impingement were measured over a wide range of Reynolds numbers [10]. Breakup and spray formation by the unlike doublet and split triplet elements were optically measured and addressed [11]. Effects of orifice geometry on the spray characteristics were examined with emphasis placed on the microscopic spray parameters [12]. Effect of the jet momentum ratio on the liquid-phase mixing of the unlike split triplet impinging injector were experimentally investigated and showed that the mixing largely depends on the secondary impingement [13, 14].

In this study, the breakup and spray formation of impinging liquid jets introduced into low-speed cross-flows are experimentally investigated. Effects of the cross-flows on the jet breakup, atomization, and spray formation are examined. The spray characteristics, including drop size, cross-sectional distribution of the drop size, penetration height and breakup length, are optically measured. Interactions between the liquid jet and the cross flow, and resultant spray formation are discussed in terms of Weber number and the momentum ratio.

2. Formation of the spray by a like-doublet impinging element

Fig. 1(a) and (b) illustrate the spray formation by a like-doublet impinging element and show an instant view of the spray profile, respectively. The impinging jets typically consist of two liquid streams which

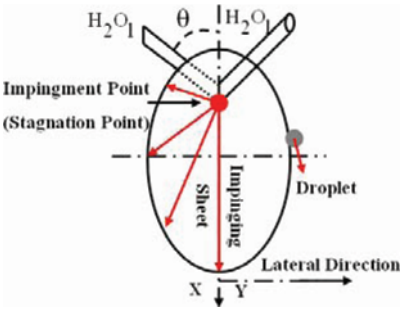

(a) Schematic of a like-doublet jet impingement and spray formation

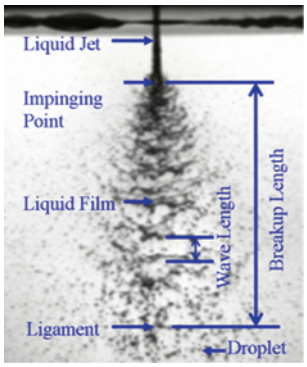

(b) A front view of spray formation due to like-impinging jets

Fig. 1. Profiles of a like-doublet jet impingement and spray formation.

collide with prescribed angle and distance from the injection surface. The impact waves originating from the jet collision give rise to the jet breakup and the atomization. The liquid sheet is disrupted while it-intermittently generates groups of drops and propagates showing wavelike expansion from the point of the impingement. A fanlike elliptical liquid sheet in the perpendicular direction to the plane of the impinging jets is formed. The like-doublet jet impingement incorporates the momentum exchanges due to both hydrodynamic and aerodynamic causes. Dissipative exchange of the jet momentum renders direct liquid-phase mixing, and the atomization takes place in an immediate after the impingement through aerodynamic interactions. A large-scale mixing of the liquids is attained by a single injection element, and a well designed impinging element yields an even spatial distribution as well as good atomization of the liquids because an additional breakup mechanism (jet impingement) gives rise to a finer spray. But the impinging jets may cause or alter the hydrodynamic stabilities because of widely banded drop size distribution [15]. In Fig. 1(b), a snapshot of the evolving spray shows that the liquid sheet breaks up and evolves intermittently into drops after the impingement. Thereinafter, the initial spray propagates, disperses or shatters into smaller drops.

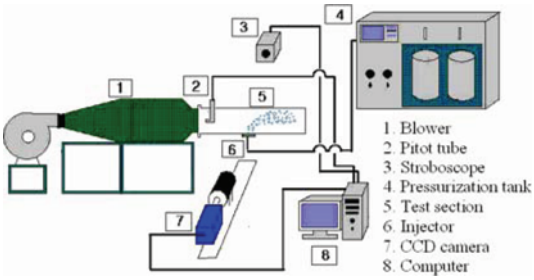

Fig. 2. Schematic of the spray test facilities.

3. Experimental setup and test conditions

Fig. 2 illustrates a test setup to measure the spray characteristics which are divided into four sections of pressurization, regulation, optical imaging and data acquisition. The apparatus is installed with a small-scale subsonic wind tunnel in which the cross-flow interacts with impinging water jets. A PC-based data acquisition system controls and records pressure, temperature, and mass flow rate. The mass flow rate is precisely maintained by advanced servo circuits in order to limit the fluctuation of pilot tank pressure.

Air is blown into the subsonic wind tunnel equipped with a test sector of a rectangular cross-section (150mm × 150mm) with its inflowing speed in the range of 10 and 50 meters per second. A pulsed shadow-graphic technique was used to capture instant images of the spray. A CCD (Charge-Coupled Device) camera (Flow-Master 3S, LaVision Inc.) is synchronized with an illumination by a stroboscope. The PTU (programmable timing unit) commands this sequence and limits the exposure duration within 15 nano seconds. Image capturing unit is saddled on a traversing rail. After taking 50 consecutive snapshot images, it shifts to the next coordinate and places the focal point of a high-power object lens onto a predetermined lattice point. Every image is stored for its analysis once the imaging is completed. Two spherical particles of the mist droplet (3μm) and the steel ball (500μm) were imaged and measured to find the reduction ration. To distinguish the presence of the droplet and measure the drop size, all images are scanned for the pixels and crude pixel data are filtered

in order to eliminate the noise in advance. When the number density of the pixels is greater than the threshold, that space is regarded as the liquid, or the gas (vapor). Once the liquid volume is recognized, its aspect ratio is calculated. The liquid volume of the aspect ratio in the range from 0.8 to 1.2 is regarded as a droplet. An arithmetic mean diameter of individual droplet is obtained and stored for next SMD calculation. To ensure highly resolved spray data with 95% confidence limits, 5,000 drops were sampled for the SMD calculation [16].

A detailed understanding of the spray dynamics in conjunction with crossing air-flows is a principal aim of the present study. To this end, parameters for inertial interaction and mutual penetration of liquid jets are examined. Essential geometric and operational parameters are summarized in Table 1.

Injection rate of the water ranges from 1.4 to 9.6 g/s or, equivalently, jet Reynolds number ($\mathrm{Re_l} \equiv \rho V_l d_0 / \mu$) approximately from 1,800 to 12,200. Here V_l and d_0 are the injection velocity and the orifice diameter, respectively. In this range of liquid jet Reynolds numbers, the liquid jet exiting the injection orifice is turbulent.

Characteristics of a plain single-orifice spray introduced into a subsonic cross-flow largely depend on the cross-flow velocity rather than transport properties of the liquid [6, 7]. Accordingly, the spray characteristics may be well expressed in terms of the flow properties rather than the fluid properties. For cross-flows, the inflowing air speed was varied in the range from 6 to 40 m/s, or equivalently, Reynolds number of the gas in the range from 400 to 2800. The air stream from a blower may be turbulent or concurrent with complicated secondary flows such as cascading flow recirculation. The air flow introduced into the duct is larminarized while it passes through a honeycomb stabilizer installed immediately downstream of the blower, hence the air-flow is laminar and carries axial momentum only. Pitot-tube tests conducted at the exit of the honeycomb stabilizer verified an occurrence of uniform cross-sectional velocity distribution with minimal spatial variations.

Table 1. Geometric and operational parameters of the unlike-doublet impinging atomizer.

Orifice diameter, d_0	0.5 mm	Gas velocity	6 ~ 40 m/s
Impingement distance	3 mm	Injection rate	1.4 ~ 9.6 g/s
Included angle	60°	Re_l	1,800~12,200
L/ d_0	6	We_l	70 ~ 5,000
Injection pressure	0.0355 ~ 0.7 MPa	Momentum Ratio, q	7 ~ 13,000

* Re_l : Reynolds number of injected liquid jet
We_l : Weber number of injected liquid jet with regard to the cross-flow velocity
L: Injection orifice length

Interrupted by strongly convective cross-flows, the drops (or the spray) quickly decelerate by the aerodynamic drag, settle down to the gas flow, and evolve into a drop-laden flow downstream. Neglecting the gravitational effect, the terminal velocity of a droplet situated in the traversing gas stream is set to be equal to that of the gas flow. A stopping time (an interval during a stagnant droplet is accelerated up to the gas velocity) is proportional to square of the droplet diameter. In the practical size range, the droplet promptly adjusts to the gas motion. At standard conditions, the stopping time for a droplet of 100 μm diameter in the cross flow of the relative velocity of 10 m/s is on the order of 10^{-2} second. The aerodynamic interaction caused by non-zero relative velocity is activated in a narrow region centered on the liquid stream, and the atomization including the secondary breakup rapidly diminishes as the spray proceeds downstream. Thus, the axial location for imaging and measuring the spray could be safely chosen as 7.5 cm downstream from the location of the jet impingement.

4. Results and discussion

The degree of atomization was estimated in terms of Weber number of the liquid jet and the liquid-to-gas momentum ratio. Weber number ($\mathrm{We_g} = \rho_g d u_g^2 / \sigma$) is defined as the ratio of momentum flux of the gas flow acting on the liquid to surface tension restraining the liquid[17]. With no presence of interrupting gas flows, the degree of atomization is a function of the ratio of a relative magnitude of activation (liquid jet momentum) to that of attenuation (surface tension). For the jet Weber number ($\mathrm{We_l} \equiv \rho_l d_0 u_l^2 / \sigma$), however, the momentum carried by the liquid jet replaces the momentum flux of the gas flow since this liquid jet momentum serves to cause an additional force which renders finer spray. Inertial effect of the cross-flow on the liquid jet breakup is estimated in terms of the momentum ratio ($q = \rho_l d u_l^2 / \rho_g d u_g^2$), which is defined as the ratio of the liquid jet momentum to that of the cross-flow, hence measuring the relative inertial strength of the

liquid jet. At higher jet Weber numbers, the hydrodynamic impact waves originating from the jet impingement and the momentum exchange are predominant. The opposite holds for the injection at lower jet Weber numbers, and the liquid-to-gas momentum ratio measures the atomization quality in this low Weber number regime. It is noted that the definition of the momentum ratio may be inappropriate in order to correctly deal with the geometry of interaction, because the direction of the liquid jet is not perpendicular to that of the cross-flow. However, in view of injection configuration of the impinging element, the momentum changes in both vertical and lateral air streams are directly proportional to that of the initial jet momentum [7]. That is, an interruption is not made in a perpendicular direction but a fraction of the vertical velocity component is unchanged. Hereinafter, the dynamics and characteristics of the spray are discussed in terms of the jet Weber number and the liquid-to-gas momentum ratio (briefly Weber number and momentum ratio, respectively). The ranges of the jet Weber number and the liquid-to-gas momentum ratio in Table 1 were calculated from the gas and jet Reynolds numbers.

4.1 Breakup and spray formation of impinging jet in still atmosphere

An impinging element is designed to cause a jet collision by which strong momentum exchange occurs and the atomization is promoted. In the course of the spray generation there are three (internal and external) forces of a hydrodynamic force before the jet collision, impact force due to the jet collision, and aerodynamic force command. Effects of the cross-flow on the promotion of atomization are better understood if the spray characteristics due to impinging jets in a stagnant atmosphere (with no cross-flows) are known a priori. This isolates the cross-flow parameters and thus helps elucidating the spray formation in view of the cross-flows. The geometric and operational parameters in Table 1 are repeatedly used except the gas velocity and the momentum ratio.

Fig. 3 shows distinctly different breakup patterns of the like-doublet impinging jets in accordance with the injection velocity [15, 17]. Such distinct changes in the spray profile are solely due to the changes in the injection velocity, equivalently, the jet Weber number. The breakup of the impinging jets is categorized into four breakup regimes of (a) closed rim, (b) periodic drop, (c) open rim, and (d) fully developed spray. Detailed descriptions on the fluid-dispersion coupling mechanism commanding each breakup regime are found in the references [15, 17]. Even in the absence of cross-flows or at lower injection velocities, the liquid stream projecting from the impingement point exhibits highly dispersive fluid motion. This hydrodynamic wave, which is concomitant with strong pressure fluctuations, is typically volumetric for continuity, and thus the aerodynamic interaction becomes decreasingly important at higher jet Weber numbers.

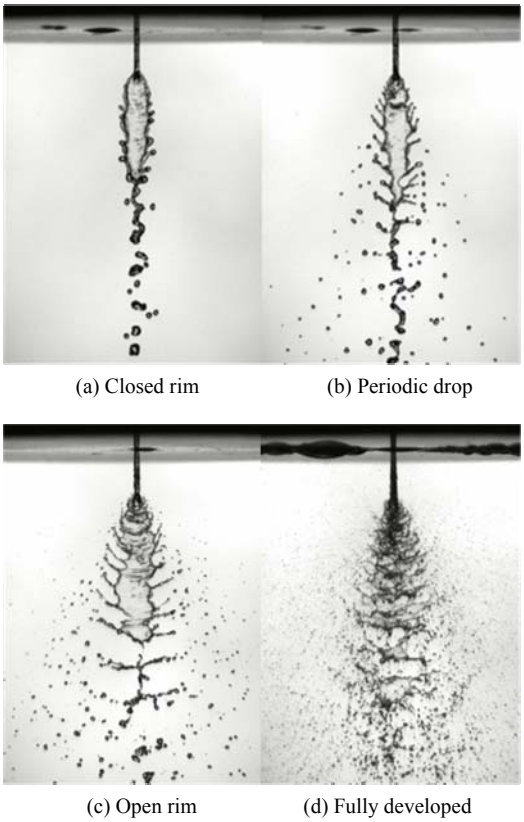

(a) Closed rim (b) Periodic drop

(c) Open rim (d) Fully developed

Fig. 3. Transition of spray pattern due to changes in the jet Weber number (We_l): (a) 299, (b) 989, (c) 2,225, and (d) 3,793).

In Fig. 4, cross-sectional distributions of SMD (Sauter mean diameter, D_{32}) manifest the inertial effects of the injection velocity (jet Weber number) on the spray characteristics. Here, SMD defined by the volume-to-surface ratio is a droplet size averaged over all drop surfaces so that it directly measures the vaporization quality. In Fig. 4, the images of the local drops were captured on the vertical cross-section at

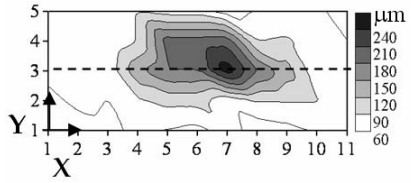

(a) We_l =1,587

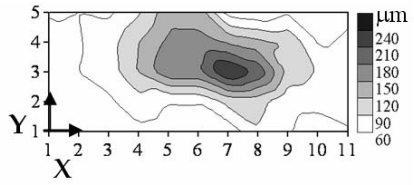

(b) We_l =2,380

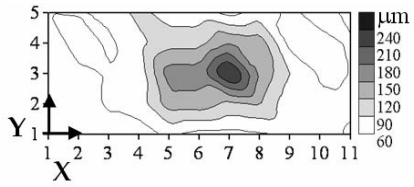

(c) We_l =3,304

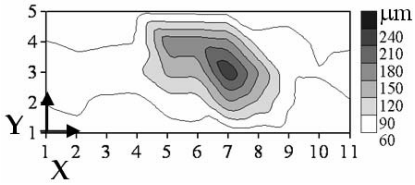

(d) We_l =3,930

Fig. 4. SMD distribution on the cross-section at 7.5 cm downstream from the impingement point (1,587<We_l<3930).

the axial distance of 7.5 cm downstream of the impingement point. As was noted previously, more than 5,000 drops were sampled in order to ensure a high resolution with the confidence limits of 95%. At all jet Weber numbers examined, the impinging jet breaks up in the regime of fully turbulent flows. In all SMD contours in Fig. 4, larger drops crowd in the spray core and the drop size progressively decreases toward the edge of the spray plume [18, 19]. Occurrence of this peculiar droplet-size distribution is caused by the formation of a liquid sheet after the jet impingement. Concomitant with the jet impingement, the liquid jets are squeezed into thick bulk liquids for continuity and stretched out into the lateral direction in order to conserve their momentum (Fig. 1(a)). Since the hydrodynamic waves after the jet impingement have long wavelengths, the drop size is proportional to the thickness of the liquid sheet. As it

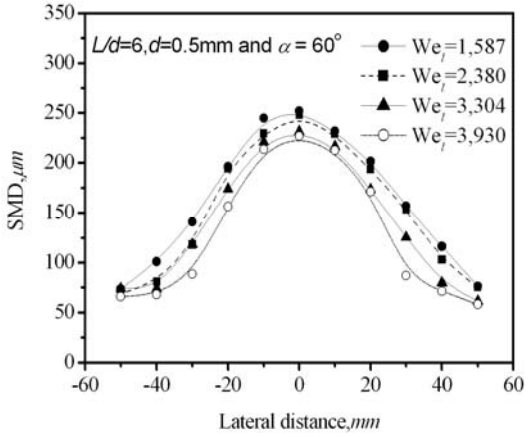

Fig. 5. Variations of SMD along the horizontal centerline to the plane of impinging jets.

stretches, the liquid sheet becomes gradually thinner for continuity and disintegrates into smaller drops.

Fig. 5 plots spatial variations of SMD at the Weber numbers in the range from 1,587 to 3,930. As expected, SMD decreases as the jet Weber number rises. Impingement of the turbulent jets at higher injection velocity induces strong impact waves, and the liquid sheet disintegrates immediately in an entire range of operating conditions. Promoted by the interaction between the liquid sheet and the atmospheric air, aerodynamic reaction amplifies the surface wave exponentially. Here the amplitude and the wave length depend on the relative velocity only. Subsequently, when the wave amplitudes arrive at their maximum, the sheet tends to breakdown at the crests and troughs in the magnitude of the half-wavelength. In view of the fact that both the wavelength and the breakup length become shorter at higher injection velocities, impact and aerodynamic disintegrations evolve similarly at these higher jet Weber numbers [17]. Since the thickening rate of the liquid sheet at an instance of the sheet breakup is less than the rate of decrease in wavelength, the drop size diminishes as the jet Weber number rises.

4.2 Breakup and spray formation due to an impinging jet in cross-flows

Snapshot photographs in Fig. 6 present a general profile of how the cross-flow alters the breakup of the impinging jet at lower injection velocity of 3.4 m/s (We_l=78). Here, the liquid-to-air momentum ratio (q) is varied within the range from 7 to 254. The liquid stream projected from an impingement point

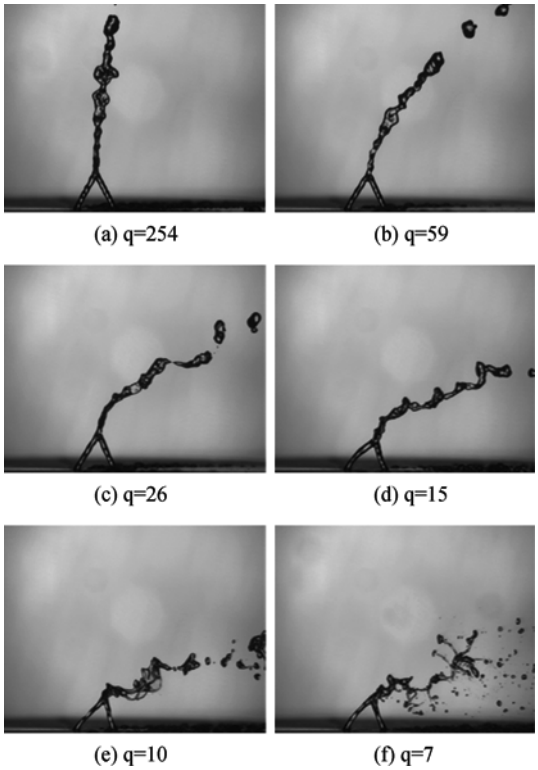

Fig. 6. Profiles of the impinging jet breakup at the Weber number of 78 (7<q<254) and the momentum-ratio from 7 to 254.

promptly stretches out laterally and forms a thin sheet in a direction perpendicular to the plane of impinging jets. In Fig. 6, only the lateral views of the jet breakup are shown because the cross-flow exerts bending force onto the face (to the right of Fig. 6) of the liquid sheet.

In Fig. 6, the jet Weber number is so low at 78 that resultant liquid stream after the jet impingement undergoes column breakup. The momentum carried by the liquid jets is not enough to induce intensive mutual penetration. This type of column breakup was previously observed in the experiment on single jet breakup assisted by gas cross-flows [20]. When the momentum ratio is 254 (Fig. 6(a)), the impinging jet overwhelms the cross-flow motion, and the profile of the liquid stream projecting from the impingement point mimics the closed-rim impinging jet breakup shown in Fig. 3(a). In this regime of lower jet Weber numbers, the liquid stream disintegrates through the mechanism of Rayleigh jet breakup. Rayleigh jet breakup is characterized by the growth of antisymmetric oscillations of the jet surface. Symmetric waves (dilatational waves) are formed in a radial direction by the interaction of primary disturbances in the liquid jets and surface tension force [21]. In other words, if the wavelength of the initial disturbance is greater than the minimum wavelength of the disturbance, the surface tension force tends to increase the disturbance, which eventually leads to a disintegration of the liquid jets. In Fig. 3(a), the dilatational waves occur immediately after the jet impingement and give rise to an initial disturbance in the liquids. The dilatational waves are then amplified through their interaction with the surface tension and, eventually, the liquid column is disrupted into drops by the inertial force at the node of the dilatational wave.

At lower momentum ratios, the aerodynamic interaction between the liquid and gas streams commands the breakup process. Interrupted by the traversing liquid stream, the uniform air-flows are hindered and are slowed down in order to redirect their streamlines for going around less mobile liquids. Reduction in the cross-flow velocity is converted into the static pressure at an immediate upstream of the liquid column. In contrast, the static pressure at the rear of the liquid sheet is lower than that at front because of viscous momentum loss. Resultant pressure drag causes bending of the liquid sheet. The lower the momentum ratio is, the larger the pressure difference. Concurrent with sheet deformation, the pressure forces interact with impact waves propagating on the liquid surface, amplify the hydrodynamic waves, and disintegrate the liquid stream. The liquid stream is flattened toward downstream in the shape of an asymmetric ellipsoid, and disintegrated at the nodes of the hydrodynamic wave. In addition, asymmetric flow geometry which causes uneven force distribution on the dilatational wave distorts the liquid sheet into a toroidal jet (Fig. 6(d)).

When the cross-flow Reynolds number is further raised into 2,055 (q=10), the liquid column undergoes bag/plume breakup (Fig. 6(e)). The bag/plume breakup is due to the concavity of the local jet geometry (Fig. 6(d)). Once swelled out by higher pressures at the front, the liquid bag continues to inflate and pops up into small drops if the pressure force becomes greater than the surface tension (Fig. 6(f)). Similar to the open rim breakup shown in Fig. 3 (c), a plume with long threads rooting on the liquid sheet disintegrates into drops.

Fig. 7 exhibits the sprays at an intermediate jet Weber number fixed at 293 and the momentum ratios

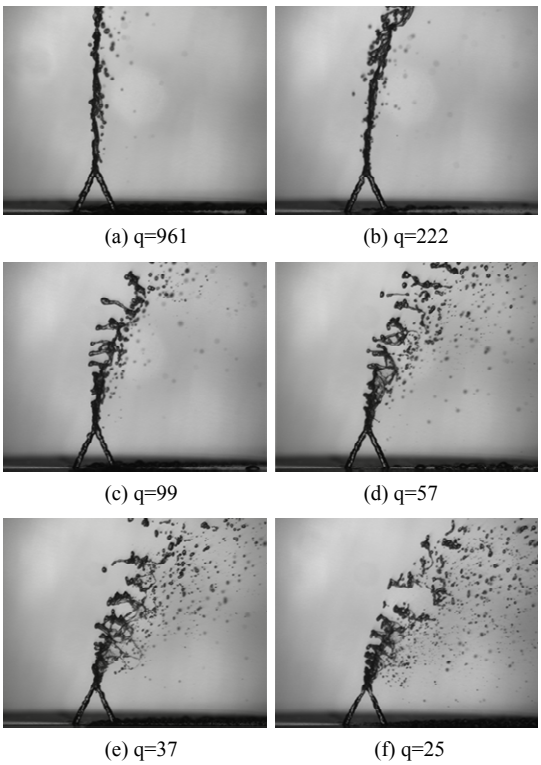

Fig. 7. Profiles of the impinging jet breakup at the Weber number of 293 and the momentum-ratio from 25 to 961.

varied in the range from 961 to 25. At higher momentum ratios (Fig. 7(a) and 8(b)), the jet breakup resembles a plain jet disintegration in the first and the second wind breakup regime [22]. The liquid after the impingement point stretches out while it forms the liquid fan (Fig. 1(a)). Lateral velocity of the stretching liquid rises in proportion to the jet collision velocity, hence the liquid fan grows wider with increasing in the jet Weber number. The spreading of the liquid sheet is due to the destruction of the jet momentum and resultant high-pressure region centered on an effective stagnation point [22]. Because of its widened contact surface, a liquid sheet of larger fan angle is more apt to be disturbed by the cross-flows. After the formation of a fan-like liquid sheet, the surface tension and the aerodynamic force compete. The liquid sheet is deformed and dispersed with an increase in the cross-flow velocity.

In Fig. 7(a), the momentum carried by the cross-flow is not strong enough to cause a column deformation and the spray shape is a vertical liquid fan where many drops crowd at its edge. This fan-like liquid sheet gets thinner from the center to the edge where the liquid stream is easily deflected by the cross-flow. An aerodynamic force overwhelms the surface tension and commands the disintegration of the liquids. This geometry of spray formation is common at all momentum ratios, and the general shape of the spray is a horseshoe pattern which is centered at the symmetry of the fan. In the vicinity of the impingement point, the force by the momentum of the liquid sheet is superior to the aerodynamic drag. An asymmetric impact wave occurs, but the amplification is not fast enough to disintegrate the thick liquid sheet, and thus the waves are progressively dissipated. In contrast, the shear forces caused by the aerodynamic interaction amplify the surface waves and rapidly disintegrate the liquids from the edge of the liquid fan. In Fig. 7(b), the momentum of the liquid stream in the neighborhood of the impingement point is still strong, but is progressively dispersed or dissipated along with enlarging liquid fan. A liquid bag occurs and ruptures into drops.

Figs. 7(c) through 7(e) show the mixed-mode (bag/plume) breakup pattern. As the cross-flow momentum rises, the breakup mechanism on the front of the liquid fan undergoes its change from that of the rear. On the front, the aerodynamic interaction is activated in proportion to the cross-flow momentum. Since undulating hydrodynamic waves caused by the jet impingement are perturbed directly by the cross-flows, the liquid sheet is progressively deformed into bags or ligaments and then ruptures. On the other hand, the cross-flow turns around the liquid fan and strong surface interaction occurs at the rear of the liquid fan due to freshly generated secondary flows. The surface waves are amplified and liquids are atomized. This unique atomization mechanism becomes more distinctive as the liquids proceed upward to the fan edge. At lower momentum ratio of 37 (Fig. 7(f)), the liquid sheet undergoes shear breakup. Wave-like surface fluctuations caused by aerodynamic drag force occur at the front of the deflected liquid sheet. This active interaction is due to an elevated jet Weber number in part. With increasing in the jet Weber number, the liquid sheet grows thinner for continuity and the spray angle augments. Kelvin-Helmholtz instability amplifies the waves rapidly and the liquid disintegration is promoted [23]. Besides, at high jet Weber numbers, the hydrodynamic waves of relatively short wave length act on the liquid sheet and give rise to the surface waves of short wavelength particularly at the edge of the spray. This concentric

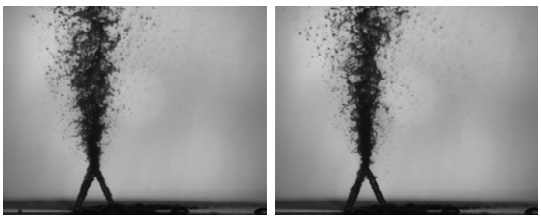

(a) q=13,169 (b) q=3,038

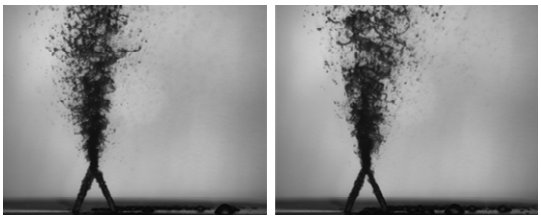

(c) q=1,357 (d) q=784

(e) q=510 (f) q=339

Fig. 8. Profiles of the impinging jet breakup at the Weber number of 4,032 and the momentum-ratio from 339 to 13,169.

wave disintegrates the liquid sheet into the ligament bands and the ligaments are progressively disrupted into the drops by shear force.

Instant spray profiles at a very high jet Weber number of 4,032 and the momentum ratios in the range from 13,169 to 339 are shown in Fig. 8. At this high jet Weber number over 4,000, the momentum of impinging jets overwhelms the aerodynamic force. The hydrodynamic impact waves command the atomization process, whereas the aerodynamic effect becomes insignificant. At momentum ratios from 784 to 13,197 (Fig. 8(a) to 8(d)), the sprays are fully developed and appear to be similar to that in Fig. 3(d). Even at lower momentum ratios of 510 and 339, the sprays are feebly bent by the cross-flows (Fig. 8(e) and 8(f)). At these higher jet Weber numbers, the spray dynamics weakly depends on the momentum ratio. In the case of the plane single jet interacting with strongly convective cross-flows, the liquid-to-gas momentum ratio is an essential parameter for the macroscopic spray characteristics such as penetration extents. However, the impinging jets interacting with

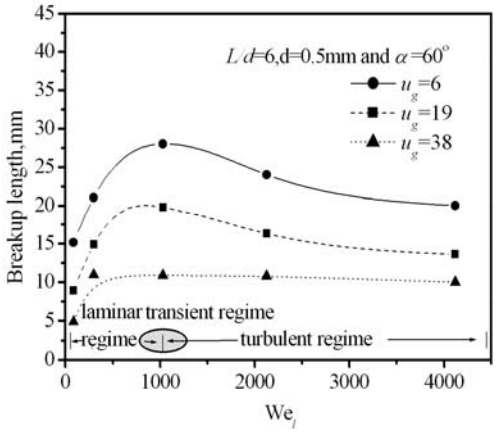

(a) Injection velocities (We_l)

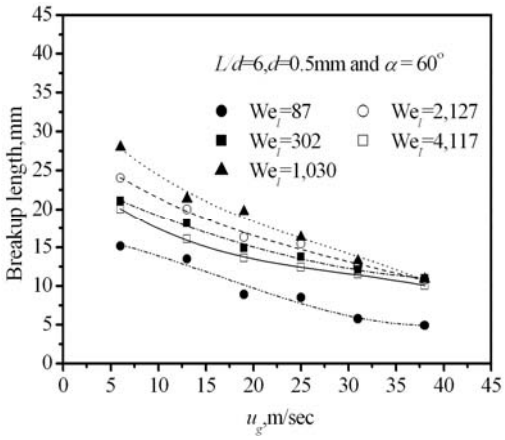

(b) Cross-flow velocities (u_g)

Fig. 9. Breakup lengths versus (a) injection velocities (jet Weber number) and (b) cross-flow velocities.

cross flows exhibit distinctly different spray profiles in a narrow range of the momentum ratios (Fig.7(a), Fig. 7(b), and Fig. 8(f)). Additional hydrodynamic jet breakup which is concomitant to aerodynamic atomization may be a plausible cause.

4.3 Cross-flow effects on the spray parameters

Macro- and microscopic spray characteristics of the like-double impinging jets in low speed cross-flows were measured. An emphasis is placed on elucidating the cross-flow effects on the atomization. When the gas stream is blocked by the liquid stream, it slows down and the momentum carried by the gas is converted into the pressure which exerts shear force on the liquids. This pressure force is partly spent to bend the liquid jet and the rest to disintegrate the liquids

through various interaction routes. In Fig. 9, plots of the breakup lengths are presented in terms of the inlet gas velocity and the jet Weber number. Here the breakup length is defined by the distance from the nozzle tip to the location where the liquid sheet is disconnected. The breakup length grows shorter at higher cross-flow velocities (Fig. 9(a)) or lower jet Weber numbers (Fig. 9(b)). Fig. 9(a) shows the breakup lengths decreasing with rising cross-flow velocities. At a given cross-flow velocity, an intact core extends in proportion to the jet Weber number and yields a longer breakup length, but shrinks as the jet Weber number rises over 1,000. This non-monotonic variation of the breakup length is relevant to the flow evolution from laminar to turbulent regime. For laminar impinging jet with the jet Weber numbers in the range from 87 to 1,030, impact waves caused by the jet impingement command liquid sheet disintegration. The impact waves attenuate rapidly as they propagate through dissipative liquids. Therefore, the completion of the breakup is retarded at lower jet Weber numbers because of weaker impact waves. In contrast, when the jet Weber number is higher than 1,030, the liquid jets enter into the turbulent flow regime. Since the turbulent eddies transport the momentum to entire liquids before the impact waves are dissipated by the smallest eddies, the impact waves are still active in the vicinity of the impingement zone and directly affect the disintegration of liquid sheet. In the turbulent flow regime, the momentum transfer is dramatically activated because the fluid particles of fluids move irregularly causing continuous exchange of momentum from one portion to another (i.e., turbulent shear stress due to the eddy structure). In addition, the turbulence causes a rugged surface that is more apt to be deformed by the aerodynamic drag. Under the present injection condition, the turbulence tends to reduce the breakup length and promote the atomization. The aerodynamic drag exerted on the liquid surface gives rise to exponentially growing aerodynamic waves whose amplitudes and waves length are related solely to the relative velocity. Thus, shrinking on the intact core is also expected to occur at higher cross-flow velocities.

Penetration by a spray is measured by the maximum distance which leading edge of the spray plume reaches, and its vertical component is frequently termed as a penetration height. The penetration height which limits the size of the inlet duct or a combustor is one of the essential geometrical design factors in conjunction with the breakup length. When the penetration exceeds the combustor height, wall-wetting and uneven mixture-ratio distribution occurs. Such

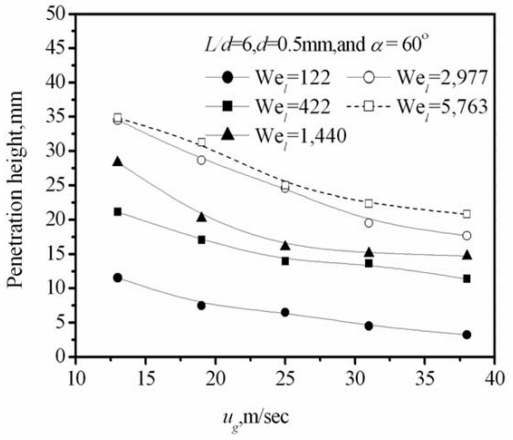

Fig. 10. Effects of the cross-flow velocity and the jet Weber number on the penetration height.

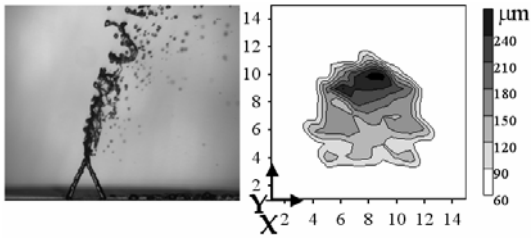

(a) q=111

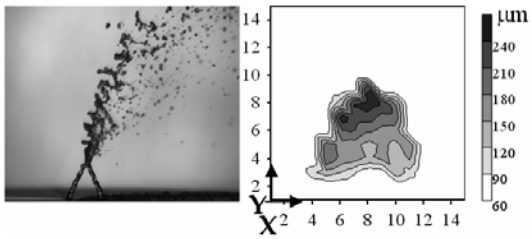

(b) q=72

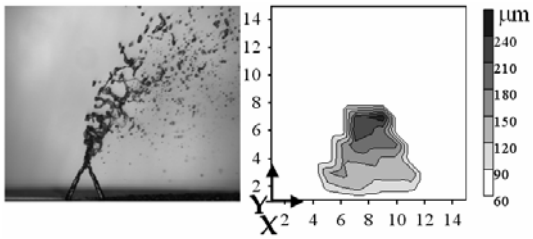

(c) q=48

Fig. 11. Profiles of spray formation by the impinging jets and iso-SMD lines on the cross section at 7.5cm downstream from the impingement point (48<q<111, We_l=573).

non-uniformity lowers the thermal efficiency and often jeopardizes the system due to seriously unbalanced thermal compatibility. In Fig. 10, the penetration height consistently drops with increasing in the cross-flow velocity. Similar to the case of breakup length, the penetration height decreases as the cross-flow velocity rises because the aerodynamic drag is squarely proportional to the velocity.

Fig. 11 exhibits lateral views of the spray and contours of the cross-sectional SMD distribution. Local SMD is optically measured at the cross-section located at 7.5cm downstream of the impingement point, which is segmented into 169 (13 x 13) squares of 10 mm height and width. A CCD camera equipped with a lens of 600 magnifications took the snapshot photograph at the focal point in the spray. The momentum ratio was varied in the range from 111 to 48 when the jet Weber number was unchanged at 573. At all momentum ratios, larger drops occur at the upper edge. The liquid jet generally consists of an inertial jet core and thin liquid sheet which surrounds the core zone. The high-velocity stream centered on the jet axis is disintegrated by a hydrodynamic cause, whereas the liquids at the edge by the aerodynamic interaction. Since an occurrence of the impact waves is a result of momentum exchange, the extent of the wave propagation is determined by the momentum mutually transported by two colliding jets. It is easily imagined that the impact at the jet periphery is less intensive because a slower and thinner liquid sheet collides there. Because SMD due to laminar impinging jets is proportional to the liquid sheet thickness [24], drops in the core zone are relatively larger and faster, henceforth these larger drops are highly inertial and penetrate deep in the cross flows (Fig. 10). In contrast, the smaller drops which are more frequent at the edge of the liquid sheet lose their momentum through viscous interaction with the cross-flow and promptly settle down to the cross-flow. Consequently, larger drops proceed farther but smaller drops outstretch broadly after the jet impingement.

The momentum transported by the cross-flow rises in proportion to the momentum ratio. In Fig. 11(a) and 11(c), the deflection of the spray is more intensive at lower momentum ratio (q=72) than higher one (q=111). Restrained by strong cross-flows, the spray shrinks and shifts toward downstream (Fig. 11(c)). At higher momentum ratios, a convex-layered spray structure develops and the penetration height is further reduced (Fig. 11(b) and 11(c)).

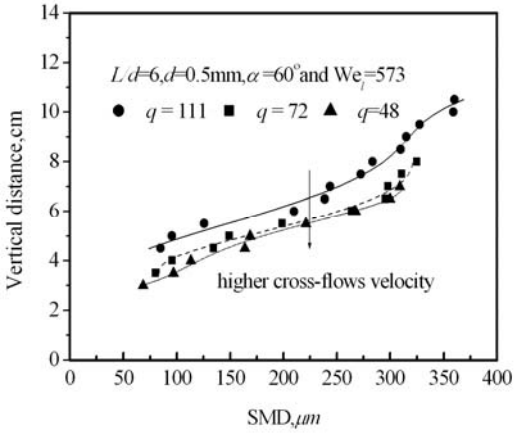

Fig. 12. Variation of SMD along a vertical direction (48<q< 111, We_l=573).

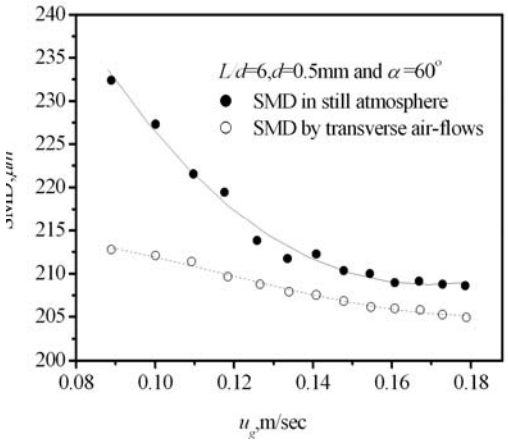

Fig. 13. Effect of the cross flow on the drop size.

Fig. 12 plots SMD variations along a vertical centerline (dotted line in Fig. 11(a)). Only the momentum ratio is changed when the jet Weber number is fixed at 573. Similar to the previous results in Fig. 11, larger SMDs occur at the upper edge of the spray plume, and this larger SMD zone shifts downstream in accordance with decreasing in the momentum ratio. Occurrence of large drops along the vertical direction is nearly monotonic at all momentum ratios. Smaller drops carry momentum that is insufficient to propel them deep into the cross-flow. These smaller drops of lower Stokes number lose their momentum and promptly settle down to the cross-flows. Consequently, small drops are crowded at lower part of the spray plume and the opposite holds for the larger ones.

Fig. 13 compares SMD variations with and without the cross-flow interruptions in terms of the cross-flow

speed. The cross-flow promotes the jet breakup and renders a finer spray in an entire range of injection velocities examined. Reduction in SMD is more substantial at lower injection velocity (higher momentum ratio) because of relatively larger momentum transfer by the cross-flow. However, the cross-flow effect on the SMD reduction no longer changes when the injection velocity rises over 0.15 m/s. In this high injection-velocity regime, the hydrodynamic impact waves command and the cross-flow contributes to secondary droplet shattering only.

5. Concluding remarks

Breakup and spray dynamics of an impinging liquid jet introduced into a low-speed cross-flow were experimentally investigated. Macroscopic and microscopic spray parameters were examined in terms of the jet Weber number and the momentum ratio, and following conclusions are drawn.

At lower jet Weber numbers, the liquid stream undergoes Rayleigh jet breakup. At higher momentum ratio, a strongly convective gas stream flattens the liquid stream of asymmetric ellipsoidal cross section, distorts the liquid sheet into a toroidal jet, and disintegrates at the nodes on an undulating liquid sheet. The liquid column undergoes bag/plume breakup through Kelvin-Helmholtz instability. In particular, the first and the second wind breakup occur at an intermediate jet Weber number. At higher jet Weber numbers, the hydrodynamic impact waves command and the effect of the convective gas flows is insignificant.

The breakup length rises in proportion to the jet Weber number, but starts to decrease when the jet Weber number further rises over 1,000. At all momentum ratios, drops are largest in the spray core and get smaller toward the edge. The cross-flow promotes the jet breakup and renders a finer spray in the entire range of injection velocities. Its effect is more distinct at lower injection velocities due to relatively stronger liquid-gas interaction.

References

[1] K. A. Sallam, H. M. Metwally and C. L. Aalburg, Deformation and surface waves properties of round non-turbulent liquid jets in gaseous crossflow, *ASME Fluid Engineering Summer Conference*, ASME Paper No. FEDSM2005-77469, Huston, TX, America, (2005) 19-23.

[2] S. J. Beresh, J. F. Henfling, R. J. Erven and R. W. Spillers, Penetration of a transverse supersonic jet into a subsonic compressible crossflow, *AIAA Journal*, 43(2) (2005) 379-389.

[3] K. A. Sallam, C. L. Aalburg and G. M. Faeth, Breakup of round non-turbulent liquid jets in gaseous crossflows, *AIAA Journal*, 42(12) (2004) 2529-2540.

[4] M. Y. Leong, V. G. McDonell and G. S. Samuelsen, Effect of ambient pressure on an airblast spray Injected into a crossflow, *J. Propul. Power*, 17(5) (2001) 1076-1084.

[5] R. P. Fuller, P. K. Wu, K. A. Kirkendall and A. S. Nejad, Effects of injection angle on atomization of liquid jets in transverse airflow, *AIAA Journal*, 38(1) (2000) 64-72.

[6] P. K. Wu, K. A. Kirkendall, R. P. Fuller and A. S. Nejad, Spray structures of liquid jets atomized in subsonic crossflows, *J. Propul. Power*, 14(2) (1998) 173-182.

[7] P. K. Wu, K. A. Kirkendall, R. P. Fuller, M. R. Gruber and A. S. Nejad, Spray trajectories of liquid fuel jets in subsonic crossflows, *7th international Conference on Liquid Atomization and Spray Systems*, Seoul, Korea, (1997).

[8] S. C. Li and K. Gebert, Spray characterization of high pressure gasoline fuel injectors with swirl and non-swirl nozzles, *SAE Technical Paper series*, California University, San Diego, USA., (1998).

[9] T. Z. Dai and G. M. Faeth, Temporal Properties of secondary drop breakup in the multimode breakup regime, *Int. J. Multiphase Flow*, 27(2) (2001) 217-236.

[10] K. Ramamurthi, K. Nandakumar and P. K. Patnaik, Characteristics of spray formed by impingement of a pair of liquid jets, *J. Propul. Power*, 20(1) (2004) 76-82.

[11] Jung Kihoon, Lim Byoungjik, Yoon Youngbin and Koo Jaye, Comparison of mixing characteristics of unlike triplet injectors using optical patternator, *J. Propul. Power*, 21(3) (2005) 442-449.

[12] Jung Kihoon, Lim Byoungjik and Yoon Youngbin, Effects of orifice internal flow on breakup characteristics of like-doublet injectors, *J. Propul. Power*, 22 (3) (2006) 653-660.

[13] Won Yeongdeok, Cho Yonho, Lee Seongwoong and Yoon Woogsup, Effect of momentum ratio on the mixing performance of unlike split triplet injectors, *J. Propul. Power* , 18(4) (2002) 847-854.

[14] Cho Yonho, Lee Seongwoong, Rhee Byungho and

Yoon Woongsup, Experimental speculation on unlike split triplet jet mixing, *41th Aerospace Science Meeting and Exhibit*, Reno, NV, USA., (2003) 322.
[15] N. Dombrowski and P. C. Hooper, A study of the sprays formed by impinging jets in laminar and turbulent flow, *J. Fluid Mech*., 18(3) (1963) 305-319.
[16] I. C. Bowen and G. P. Davies, Report ICT 28, *Shell Research Ltd*., London, UK., (1951).
[17] Kim Kyuhong, Spray characteristics of the impinging injector in the strongly convective crossflow, *Ph. M.thesis*, Yonsei University, Seoul, Korea, (2004).
[18] H. M. W. E. Anderson, W. E. Rhan, S. Pal and R. J. Santoro, Fundamental studies of impinging liquid jets, *30st Aerospace Sciences Meeting and Exhibit*, Reno, America, (1992).
[19] H. H. Foster and M. F. Heidmann, The spatial characteristics of water spray formed by two impinging jet at several jet velocities in quescent air, *NASA TND-301*, (1960).
[20] Park and Seok, Phenomena of liquid jet breakup in high speed gas stream, Journal of ILASS-Korea, 1(2) (1996) 66-73.
[21] R. D. Reitz, Atomization and other breakup regimes of a liquid jet, Ph. D. Thesis, *Princeton University*, NJ, (1978).
[22] A. H. Lefebvre, Atomization and sprays, 2nd ed., *Hemisphere, Philadelphia*, PA, (1989).
[23] G. D. Crapper, N. Dombrowski, W. P. Jepson and G. A. D. Pyott, A note on the growth of Kelvin-Helmholtz waves on thin liquid sheets, *J. Fluid Mech. Digital Archive*, 57(4) (1973) 671-672.
[24] N. K. Rizk and A. H. Lefebvre, Influence of liquid film thickness on air-blast atomization, *Trans. ASME J. Eng. Power.*, 102 (706)

Woong-Sup Yoon is a Professor in the School of Mechanical Engineering at Yonsei University. His current research interests are in wave instabilities, unusual spray formation, emission control, and propulsion system modeling. He received a BS degree from the Department of Mechanical Engineering, Yonsei University, in 1985; an MS degree from the Department of Mechanical Engineering, University of Missouri-Rolla, in 1989; and a Ph.D degree from the Department of Mechanical and Aerospace Engineering, the Unversity of Alabama in Huntsville, in 1992.

Sang-seung Lee received his B.S. degree in Weapons Engineering from Korea Military Academy, Korea, in 2002. He then received his M.S. degrees from Yonsei University, in 2006. Mr. Lee is currently a Lecturer at the School of Weapons Engineering at Korea Military Academy in Seoul, Korea. He serves as an Editor of the Journal of Mechanical Science and Technology. Mr. Lee's research interests include Ramjet, Atomization of injector.

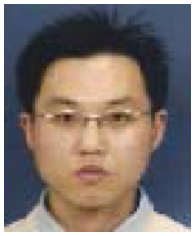

Won-ho Kim received his B.S. degree in Mechanical Engineering from Yonsei University, Korea, in 2003. Mr. Kim has then gone on to do graduate work at the Ph.D in the School of Mechanical Engineering at Yonsei University in Seoul, Korea. Mr. Kim's research interests include Atomization of 2phase flow and Dust collection efficiency.